Phase Equilibria and Structural Properties of Thiophene/[Bmim][BF4]: A Molecular Insight from Monte Carlo Simulations

Yongping Zeng, Chunfeng Wang, Junmei Hu, and WenLin Xu
College of Chemistry and Chemical Engineering, Yangzhou University, Yangzhou, 225002, China

Yueyang Xu
GuoDian Science and Technology Research Institute, Nanjing, 210031, China

Shengui Ju
The State Key Laboratory of Materials-Oriented Chemical Engineering, Nanjing University of Technology, Nanjing, 210009, China

DOI 10.1002/aic.14566
Published online August 1, 2014 in Wiley Online Library (wileyonlinelibrary.com)

The phase equilibria of thiophene in 1-butyl-3-methylimidazolium tetrafluoroborate ([Bmim][BF_4]) is calculated by Monte Carlo simulation in Gibbs ensemble using a united atom force field. The liquid density of studied ionic liquid and the vapor pressure of thiophene in [Bmim][BF_4] were compared with corresponding experimental data reported in the literature, and a good agreement was obtained. In order to describe the solubility of thiophene in this ionic liquid, we have calculated the radial distribution functions and spatial distribution functions of thiophene/IL mixtures to study the interaction of thiophene with cations and anions of [Bmim][BF_4] in the liquid phase. The local composition concept in fluid was also examined to give further insight into the liquid structure. The results show that thiophene is well organized around the terminal carbon atom of the butyl or methyl chain attached to the imidazolium ring of cations and tends to adopt a symmetrically distribution on the anions. © 2014 American Institute of Chemical Engineers *AIChE J*, 60: 3916–3924, 2014
Keywords: ionic liquid, thiophene, molecular simulation, phase equilibrium

Introduction

Due to increasingly strict environmental regulations designed to reduce sulfide emissions from combustion engines, it is very urgent for refiners to process feedstock with greater levels of sulfur.[1,2] Additionally, future fuel cells will also require the deep desulfurization of fuels, since sulfur must be further reduced to zero sulfur content to avoid poisoning and deactivating the reformer catalyst.[3] So, the removal of sulfur-containing compounds is a very important operation in petroleum refining, which is achieved by catalytic processes at elevated temperatures and pressures. Conventional hydrodesulfurization (HDS) catalysts have been highly effective for the removal of sulfur. However, the HDS process is less effective for thiophene and its derivatives.[4] It needs to further improve the HDS efficiency by increasing severe operating conditions, such as temperature or pressure. In addition, severe conditions will result in energy consumption and increased hydrogen consumption. As a result, it is difficult to use the HDS process to reduce the level of sulfur content enough to meet with the strict regulations. The extraction of sulfur compounds from the fuels instead of reaction could help to reduce energy consumption.

In recent years, room temperature ionic liquids (rILs) have been extensively evaluated as environmentally friendly and "green" solvents for the widespread applications. Many rILs show some unique characteristics that distinguish them from conventional organic solvents, such as high viscosity, low melting point, nonflammability, and negligible vapor pressure. These liquids exhibit a wide liquid range and thermal stability, and are good solvents for a wide range of inorganic or organic compounds.[5,6] Some attempts to develop an extraction process of sulfides from fuels have been performed by some researchers using rILs.[7,8] Some reports have been found that rILs can effectively remove a large amount of sulfur-containing compounds from fuel oils, such as thiophene and its derivatives.[9–11] Among these ionic liquids (ILs) studied, those based on imidazolium cations showed high efficiency for the extraction of compounds containing organic sulfur. Bösmann and Eßer et al.[8,12] studied desulfurization performance of some rILs, and found that the size of the ions is very important for the extraction desulfurization. Zhang et al.[13] compared the absorption capacities of [Emim][BF_4], [Bmim][BF_4], and [Bmim][PF_6] for some model fuel, and further elucidated the structural effects of rILs on the extraction capability for thiophene by

Additional Supporting Information may be found in the online version of this article.

Correspondence concerning this article should be addressed to Y. Zeng at ypzeng@yzu.edu.cn.

multinuclear magnetic resonance (NMR) spectroscopy. Nie and coworkers[7,14] reported *N*-methylimidazole- and *N*-ethylimidazole-derived dialkylphosphate rILs showed good extraction desulfurization ability for fuel oil. Nie et al.[15] also reported the extractive performance of three phosphoric rILs for the sulfur compounds 3-methylthiophene, benzothiophene, and dibenzothiophene (DBT) from gasoline. Mochizuki et al.[16] investigated six types of halogen-free ILs with different alkyl chain lengths and evaluated the extraction yield of DBT compared with that of diphenylsulfide and diphenyldisulfide. The results show that the extraction yield of DBT increased linearly with an increase in the length of alkyl chains.

Three types of pyridinium-based ILs were examined to be effective for the selective removal of aromatic heterocyclic sulfur compounds from diesel at room temperature by Gao et al.[17] Their results showed that the structure and size of the cation greatly affect the extractive performance of rILs. The performance in extraction desulfurization of some rILs that are composed of anions such as $[BF_4]$ and $[PF_6]$ and popular cations of imidazolium and pyridinium has been explored, and the results are fairly good. Although ILs have the potential for applying to these separation process, the thermodynamic data containing IL systems is scarce, which hindered their applications. Vapor-liquid equilibrium (VLE) data for systems containing ILs are important for separation, and they are essential for design of the operation and optimization of chemical processes. Conversely, in order to have a better insight into the structure–property relationship of this series of rILs with respect to the extractive desulfurization, more theoretical insights are required. Efforts have been made using theoretical methods to simulate rILs. Kumar and Banerjee[18] used the quantum chemical-based Conductor like Screening Model for Real Solvents (COSMO-RS) predictions to evaluate the performance of 264 possible rILs in the removal of thiophene from diesel oil. Based on similar methods, Anantharaj and Banerjee[19] used COSMO-RS to predict the nonideal liquid-phase activity coefficient for mixtures containing 1-ethyl-3-methyl imidazolium thiocyanate [Emim][SCN], heterocyclic compounds, and water. Anantharaj and Banerjee[20] used the nonrandom two liquid (NRTL) and Universal Quasi-Chemical (UNIQUAC) models to study the separation of thiophene from model oil with 1-ethyl-3-methylimidazolium acetate [Emim][OAc], 1-ethyl-3-methylimidazolium ethylsulfate [Emim][$EtSO_4$], and 1-ethyl-3-methylimidazolium methylsulfonate [Emim][$MeSO_3$] as the extraction solvents. Extraction of thiophene from *n*-heptane using ILs was modeled by both NRTL and UNIQUAC approaches to correlate with the experimental results.[21] Anantharaj and Banerjee[22] performed the natural bond orbital analyses to investigate the interactions of thiophene and pyridine with different ILs, which include 1-butyl-1-methyl pyrrolidinium tetrafluoroborate ([Pyr14][BF_4]), 1-butyl-1-methyl pyrrolidinium hexafluoro-phosphate ([Pyr14][PF_6]), 1-butyl-4-methyl pyridinium tetrafluoroborate ([BPY][BF_4]), 1-butyl-4-methylpyridinium hexafluorophosphate ([BPY][PF_6]), and 1-benzyl-3-methylimidazolium tetrafluoroborate ([BeMIM][BF_4]). Su et al.[23] performed NMR spectroscopy to study the interactions between thiophene and the ILs of 1-butyl-3-methylimidazolium hexafluorophosphate ([Bmim][PF_6]) and 1-butyl-3-methylimidazolium tetrafluoroborate ([Bmim][BF_4]). Revelli et al.[24] used NMR and thermodynamic analysis to study the interactions between thiophene and benzene molecules with three imidazolium ILs. NMR study shows that solubility of thiophene or benzene in IL strongly depends on the structure of the IL. Zhou et al.[25] performed *ab initio* calculations to examine the interaction of thiophene and imidazolium-based ILs with BF_4 or PF_6 anions. The optimized structures show that the anions of the ILs are situated outside the ring plane of the thiophene, with the fluorine atoms interacting with the hydrogen atoms of the thiophene. In addition, the cations of the ILs approach the thiophene with their positively charged atoms approaching the negatively charged atoms of thiophene.

However, so far the studies performed with various rILs did not draw any concrete conclusion or trend. Moreover, the detailed structures and conformations of interactions between thiophene and rILs in liquid phase, which are rather important in understanding their physical properties, are still not clear. Thus, we still need a clear awareness of the liquid-phase structural properties of mixtures and interactions between thiophene and room temperature ILs. We expect that computer simulations can provide an alternative way in screening a large number of candidate room temperature ILs to absorb thiophene from fuel oil efficiently. Among the numerous synthetic rILs known to date, as a case, [Bmim][BF_4] is widely studied and commercially important. The model system was not previously performed for absorption of thiophene in [Bmim][BF_4] and it is also an obvious benefit to being able to predict properties of sulfur-containing compounds with computational methods. The theoretical results here will help to understand the fundamental interactions between thiophene and [Bmim][BF_4].

Force Fields and Simulation Details

In this work, for [Bmim][BF_4] IL, a standard molecular mechanics force field is used, with functional form

$$\begin{aligned} U_{\text{total}} &= U_{\text{VDW}} + U_{\text{qq}} + U_{\text{torsion}} \\ &= \sum_{i=1}^{N-1}\sum_{j>1}^{N}\left\{4\varepsilon_{ij}\left[\left(\frac{\sigma_{ij}}{r_{ij}}\right)^{12}-\left(\frac{\sigma_{ij}}{r_{ij}}\right)^{6}\right]+\frac{q_i q_j}{4\varepsilon_0 r_{ij}}\right\} \\ &+ \sum_{\text{dihedrals}}\left[\kappa_0+\kappa_1(1+\cos(\phi)+\kappa_2(1-\cos(2\phi)+k_3(1+\cos(3\phi)\right] \end{aligned} \tag{1}$$

where U_{total} and U_{torsion} are the total energy of the system and internal rotation energies of dihedral angles, respectively, r_{ij} is the distance between sites i and j, q_i and q_j are the partial charges on the sites, ε_0 is the permittivity of vacuum and σ_{ij} and ε_{ij} are Lennard–Jones parameters, κ_i and φ are the torsion angle and potential parameters.

Potential parameters for the [Bmim] cation and [BF_4] anion were taken from Maginn and coworkers and Andrade et al., respectively.[26,27] The force fields greatly reduce computational cost, and can be used to simulate larger and more complex system due to the use of united atom model. In addition, the force field parameters were determined on the basis of a large number of accurate experimental data, especially phase equilibrium data, so it is very accurate for the calculation of the thermodynamic properties, and can be used in wide temperature and pressure range. Lennard–Jones parameters for unlike atom sites are obtained using the Lorentz–Berthelot combining rules. Fixed partial charges on the united atom sites are used to calculate the Coulombic interactions. The partial charges for IL were taken from Andrade et al.[27] The [BF_4] anion was described using a five-site

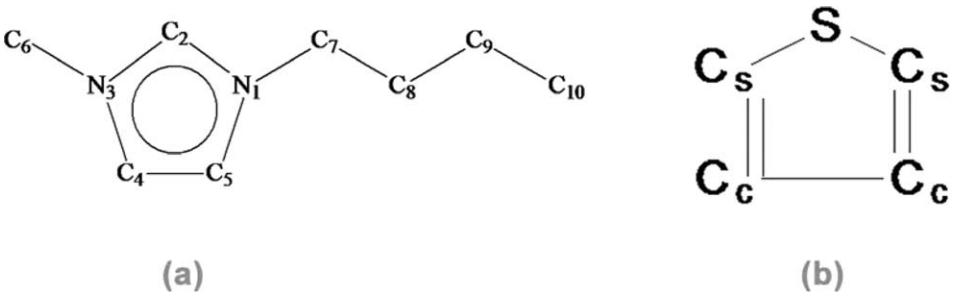

Figure 1. Atom numbering scheme of (a) [Bmim] and (b) thiophene.

model with the boron and fluorine interaction sites located at the respective atomic centers and the atom numbers of [Bmim] cation is shown in Figure 1a.

Thiophene molecule was described with a five-site united atom model and was modeled as a rigid and planar molecule (Figure 1b). The bond lengths of C—C and S—C were fixed at 1.40 and 1.72 Å, respectively. The force field parameters were taken from transferable potentials for phase equilibria–united atom (TraPPE-UA) force field developed by Lubna et al.[28] All parameters used in this work can be found in Supporting Information Tables 1S–3S.

The MCCCS Towhee code [29], which uses the GEMC method in Gibbs ensembles, was used for all simulations. Monte Carlo simulations in the isobaric–isothermal (NPT, where N is number of molecules, P is pressure, and T is temperature) ensemble were used to determine the density and radial distribution functions (RDFs) for pure IL [Bmim][BF_4]. The system consisted of 150 randomly arranged ion pairs in a cubic simulation box. Simulations were run 2×10^5 Monte Carlo cycles for production, after the initialization of 2×10^5 Monte Carlo cycles, where one cycle corresponds to N molecules Monte Carlo moves. The simulations in the NVT (where N is number of molecules, V is volume, and T is temperature)-Gibbs ensemble were performed for pure thiophene. The system consisted of 300 thiophene molecules in two separated simulation boxes. Simulations were run for 1×10^5 Monte Carlo cycles, after the initialization of 1×10^5 cycles.

For [Bmim][BF_4]/thiophene binary mixture systems, the simulations were performed in the NVT-Gibbs ensemble using a configurational-bias Monte Carlo (CBMC) technique for solutions of 40 and 59.95 mol % thiophene in [Bmim][BF_4] at the different temperatures. In order to reproduce the experimental phase equilibrium curves, the molar fractions were chosen according to the experimental compositions. The solutions consisted of 250 thiophene molecules and 300 [Bmim][BF_4] ion pairs for 40 mol % and 250 thiophene molecules and 167 [Bmim][BF_4] ion pairs for 59.95 mol %, respectively. To be sure of thermodynamic equilibrium, the simulations were run 2×10^5 Monte Carlo cycles for production, after the initialization of 4×10^5 Monte Carlo cycles. During these pre-equilibration runs, the maximum allowable translations, rotations, and volume displacements were updated every 10 cycles for the first 1000 cycles, to yield acceptance rates of approximately 50% for each move type.

The standard periodic boundary conditions were applied to all the simulated systems. Electrostatic interactions were computed using the Ewald summation method[30] with the permittivity of the surrounding medium set to 1.0, an Ewald screening parameter $K \times L = 5$, and $K_{max} = 5$ for the upper bound of the reciprocal space summation. A spherical cutoff was set to half the box length for Lennard–Jones interactions. Standard long range corrections were applied beyond the cutoff distance. The coupled–decoupled CBMC technique was used for conformational changes.[31] A hard sphere cutoff was used to immediately reject any move bringing two atoms closer than 1 Å. The ratio of moves was 19% CBMC particle swap moves between phases or CBMC identity switches(including the ion pairs of IL and thiophene), 1% volume moves, and 30% molecule translations, 30% molecule rotations, and 20% conformational moves.

Results and Discussion

Pure [Bmim][BF_4]

The density of the pure [Bmim][BF_4] was obtained as an ensemble average during NPT simulations at 101.325 kPa. Table 1 shows the numerical results of the densities. At each different temperature, the force fields predict that the densities are lower than the experimental values around 3%. This level of agreement indicates a reasonable accuracy, considering that used a combination of different resources of force field parameters for the IL and the force field parameters were not refined to reproduce the experimental densities. Shah et al.[26] performed a Monte Carlo simulation study for 1-butyl-3-methylimidazolium hexafluoro-phosphate([Bmim][PF_6]) IL using the same force fields parameters of cation with that of our work. Although the anion was different, a similar underestimation for density was also observed by them. They concluded that the reduction in net charge results in a weakening of the electrostatic attraction between the cation and anion, and then a reduction in the density. The density values were reported by Prado and Freitas[36] with an all atom molecular dynamics simulation at 300 K and 1 atm. The average density obtained by them, 1.178 g/mL, is higher than that of our work. It is much closer to experimental data compared to our simulated value, but still lower than the experimental density. The all atom force field may indicate that the explicit hydrogen atoms on the imidazolium ring and alkyl groups are necessary to capture subtle packing

Table 1. Comparison of the Densities Calculated in this Work with Experimental Data at Different Temperatures

	ρ (g/mL)	
T (K)	This Work	Experimental Data
298	1.162	1.202[32]
300	1.160	1.20[33] and 1.17[34]
323	1.152	1.184[35]
343	1.143	1.170[35]

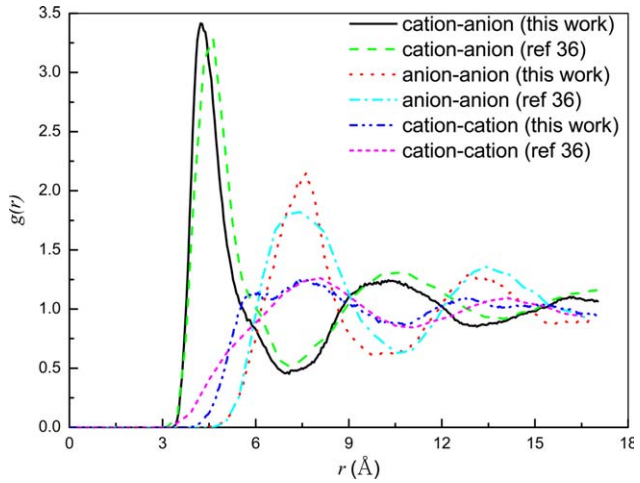

Figure 2. Radial distribution function involving cation–cation, anion–anion, and cation–anion interactions.

The reference sites are the nitrogen N1 for cation and the Boron atom for the anion according to Ref. [36]. [Color figure can be viewed in the online issue, which is available at wileyonlinelibrary.com.]

effects for this liquid. Thus, the all atom model can reproduce the experimental density much closer.

In order to test the validity of force fields for this IL, we also calculated the various RDFs for the pure IL systems. The RDFs for cation–cation, cation–anion, and anion–anion pairs at 300 K and 101.325 kPa are shown in Figure 2. To compare with RDFs in this work, we also show the RDFs of literature in Figure 3.[36] Prado et al. applied the molecular dynamics method to investigate the thermodynamics and structural properties using the all atom OPLS-AA force fields. Despite the different force field parameters, only small differences are observed in the calculated structural properties. The RDFs at other temperatures are qualitatively very similar and are not shown here. We can observe that the first peak is at about 4.5 Å for cation–anion pairs. The second peak occurs at 9.7 Å. The first and second peak positions are in good agreement with Prado et al. We also can see a weak ordering beyond 15 Å considering the long-range Coulombic interactions in this system, which are observed by some literatures.[38,39] The first and second peaks in the cation–cation and anion–anion RDF show a good agreement with results reported by Prado et al. These results show that the force field parameters for IL are reasonable in this work and can be used in the simulations of mixtures.

Pure thiophene

The pure thiophene saturated vapor and liquid densities predicted by the TraPPE-UA force fields are shown in Figure 3. To validate the accuracy of models, a comparison with the literature for thiophene's vapor-liquid is shown in Figure 3a. The saturated vapor pressure vs. inverse temperature curves are shown in Figure 3b. The TraPPE-UA thiophene model can reproduce the experimental data. It appears that the critical temperature is overestimated by about 4%, which was observed by Lubna et al.[28] using the force field parameters. It convinced us that the chosen force fields are accurate enough for the further study, such as mixtures.

[Bmim][BF4]/thiophene systems

The knowledge of the liquid-phase equilibrium is fundamental for the ILs to be effectively used as solvents in extractive distillation or liquid-liquid extraction. Phase equilibrium data of mixtures containing ILs is very important for achieving the industrialization of ILs. The thermodynamic properties and behaviors of mixtures containing ILs are required for the development of new process. To validate the accuracy and consistence of the model for thiophene and IL, the VLE for binary systems containing ILs was simulated in the NVT-Gibbs ensemble and the vapor pressure data of mixture was calculated. The pressure–temperature diagrams for the binary system thiophene/[Bmim][BF_4] at two different compositions obtained from calculations are compared to the experimental vapor pressure in Figure 4. The force fields reproduce the shape of the experimental curve well, but slightly overestimate the vapor pressure of thiophene.

With the increasing thiophene mole fraction, the deviations become larger, but are smaller than 5% in most cases. The deviations exist mainly due to the force field parameters, which overestimated the vapor pressure for thiophene. But, there is still reasonably good agreement with experiment, especially considering the well-known difficulty in computing pressures from an atomistic simulation. The force fields were, therefore, used to compute the structural properties for which experimental data do not yet exist.

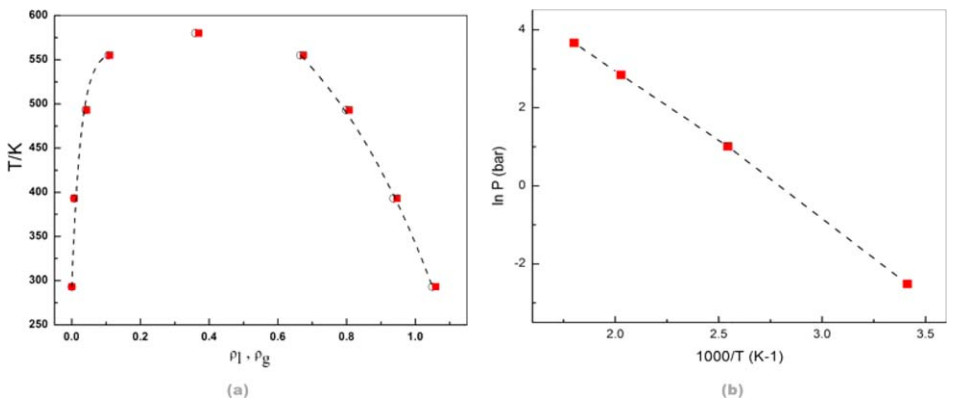

Figure 3. Vapor-liquid coexistence (a) and saturated vapor pressure vs. inverse temperature (b) curves for pure thiophene.

Circles are the data of literature.[28,37] Squares are the simulated data in this work. The lines were drawn to guide the eyes. [Color figure can be viewed in the online issue, which is available at wileyonlinelibrary.com.]

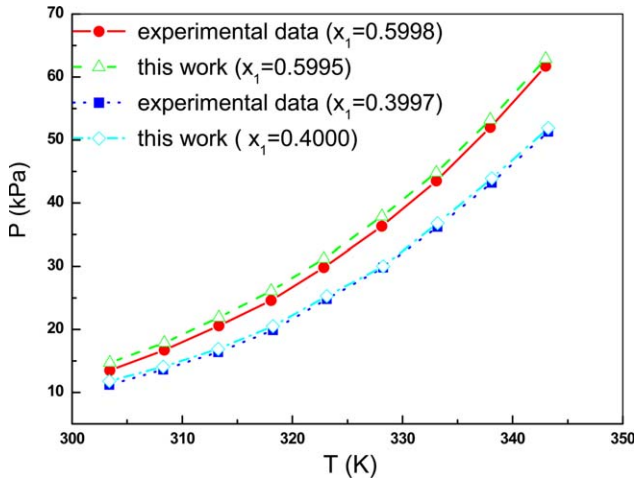

Figure 4. Comparison of vapor pressure data of the calculated and experimental data[40] for thiophene/[Bmim][BF4] mixture at different compositions.

[Color figure can be viewed in the online issue, which is available at wileyonlinelibrary.com.]

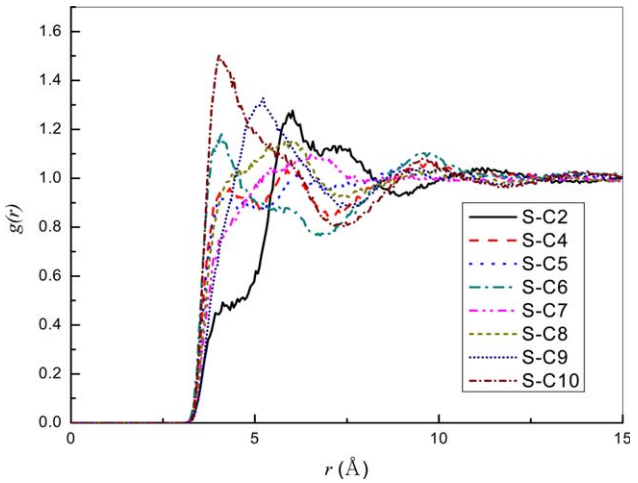

Figure 5. Radial distribution functions between carbon atoms of cation around Sulfur atom of thiophene thiophene-[Bmim][BF4] binary system of xi = 0.6 at 318 K and 21.9 kPa.

[Color figure can be viewed in the online issue, which is available at wileyonlinelibrary.com.]

Through investigation of Figure 4, it is obvious that vapor pressure decreases with a decreasing mole fraction of thiophene. As the temperature rises, the vapor pressure increases. At the range of temperatures and pressures, the relationship between vapor pressure and temperature of binary system is similar to the pure solvent vapor pressure behavior due to the nonvolatility of IL.

Fluid structure

Information on the fluid structure of the thiophene binary system included IL is rarely understood, but RDFs analysis can effectively show the fluid structure. To obtain a better understanding of the structure of thiophene in [Bmim][BF_4] solutions, the RDFs of atoms of thiophene with IL were calculated at 318 K and thiophene mole fraction 0.6. The RDFs at other mole fractions and temperatures are qualitatively very similar and are not shown here.

For the pure alkylimidazolium ILs, a nanometer scale separation into continuous and semicontinuous domains of polar and apolar regions has been observed according to some theoretical and experimental observations.[41] The high-charge density regions composed of the cationic head groups and the anions and low-charge density regions of alkyl side chains aggregate together.[42,43] The polar parts constitute continuous domains because of the high cohesive energy of the charged groups of cations and anions. The apolar regions are composed of semicontinuous domains with the side chains. In mixtures of [Bmim][BF_4]-thiophene, as expected, thiophene molecules are solvated in the apolar domains due to the much weaker polarity and do not interact with the charged group strongly.

The RDFs of thiophene atoms around carbon atoms of the cation are presented in Figures 5–7. In Figure 5, there is a highest intensity peak for the S-C10 pair RDFs compare to the other carbon atoms of IL. It is observed that the first solvation shell for the S-C10 pair peaks is at about 4.03 Å, and the second solvation shell for this pair occurs at about 9.53 Å. The results show that the thiophene prefers to associate with the C10 carbon of the side chain. It can be noticed that thiophene is well organized around the terminal carbon atom of the butyl chain attached to the imidazolium ring. From these observations, we can conclude thiophene molecules prefer to locate around the terminal carbon atom of the butyl chain. It should be expected that thiophene interacts more strongly with this part of the cation because the side chain composed of the apolar domain. However, the atoms at the ring of the imidazolium cation (except the C4 and C5) as well as the carbon C6 from the methyl group show also significant interactions with thiophene. The RDFs of thiophene sulfur atom around C6 and C10 are similar except for the peak intensity. All of these RDFs exhibit the first peak at about 4.03 Å and the second peak at about 9.5 Å. It can be noticed that thiophene is well organized around the terminal carbon atom of the butyl or methyl chain attached to the imidazolium ring. From the peak intensity, thiophene prefers to associate with the C10 carbon of butyl chain.

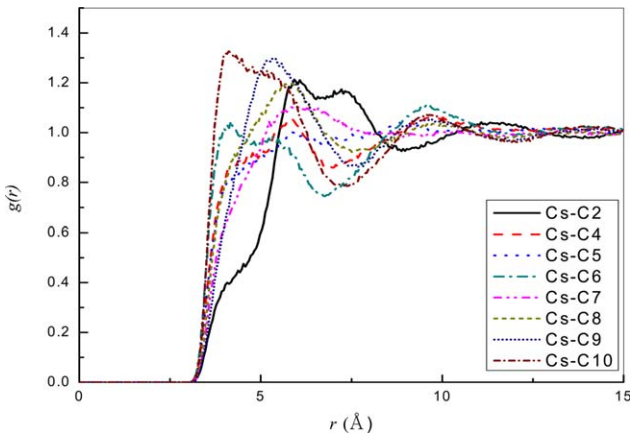

Figure 6. Radial distribution functions between carbon atoms of cation around carbon atoms of thiophene connected with sulfur atom in thiophene-[Bmim][BF4] binary system of xi = 0.6 at 318 K and 21.9 kPa.

[Color figure can be viewed in the online issue, which is available at wileyonlinelibrary.com.]

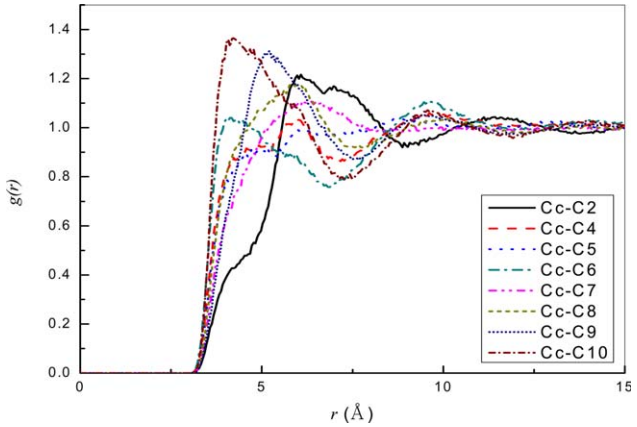

Figure 7. Radial distribution functions between carbon atoms of cation around carbon atoms of thiophene connected with carbon atoms in thiophene-[Bmim][BF4] binary system of xi = 0.6 at 318 K and 21.9 kPa.

[Color figure can be viewed in the online issue, which is available at wileyonlinelibrary.com.]

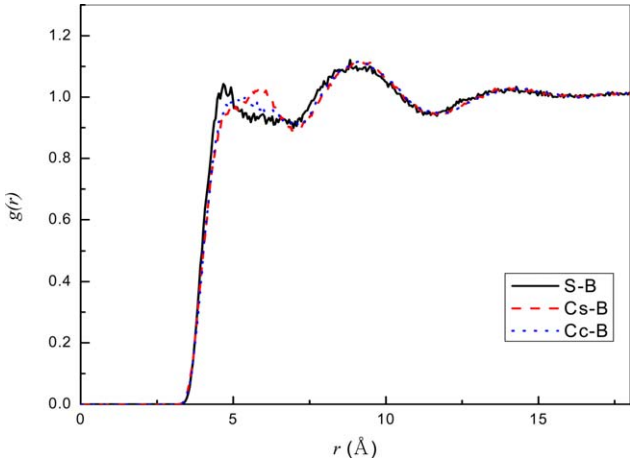

Figure 8. Radial distribution functions between boron atom of anion around thiophene atoms in thiophene-[Bmim][BF4] binary system of xi = 0.6 at 318 K and 21.9 kPa.

[Color figure can be viewed in the online issue, which is available at wileyonlinelibrary.com.]

Since the bulk of the positive charge on the [Bmim] cation is located at the C2 position,[44] interactions of [Bmim] with the [BF_4] were mainly through the C2 atoms. The sites of the cation were then responsible for the cohesion of the charged network. So it is not surprising that the first solvation shell for the S-C2 pair peaks occurs at about 5.93 Å.

The RDFs of carbon atoms of thiophene around carbon atoms of the cation are presented in Figures 6 and 7. There are not significant differences between the shapes of the RDFs for the two different types of carbon species. It is observed that the first and second peak positions for the Cc-C10 and Cs-C10 pairs are very similar. Compared with S-C10 pair, the peak intensity of Cc-C10 and Cs-C10 RDFs is lower. The RDFs show a more specific orientation of the thiophene around C10 atom, with a preferable orientation to sulfur atom of thiophene, suggesting more favorable interactions with the sulfur atom than with the carbon atoms of thiophene.

The RDFs of thiophene atoms around boron atom of anion are shown in Figure 8. Figure 8 shows that RDFs has a relatively higher and sharper peak of the first peak for sulfur atom of thiophene comparing to carbon atoms, although the height of the first peak are all close to 1, which shows a very weak ordering. It shows that it has a relatively high probability to surround the sulfur atoms of thiophene than to surround the carbon atoms. While, there is a similar second peak for the three types of atom pairs. The second peak is much stronger and broader than the first peak. It suggested that there was an ordered secondary structure at about 8.8 Å for the three types of atom pairs. Figure 8 also shows that the first peaks for the S–B pair in [Bmim][BF_4] are lower than the corresponding peaks in Figure 5, indicating that the thiophene localizes more strongly with the [Bmim] cation than with the [BF_4] anions.

Local compositions in fluid can be examined to give the further insight into liquid structure.[45] Accurate prediction and understanding of thermodynamic properties and fluid structure of electrolyte solutions is of extreme importance in development of accurate activity coefficient models and the local composition can provide valuable insight into the organization structure of fluid mixtures.[46,47] To compute the local composition within a sphere of radius r, we can define the coordination number of species j with respect to a species of type i as

$$N_{ij}(r) = \frac{4\pi N_i}{V}\int_0^r g_{ij}(r) r^2 dr$$

where N_i is the number of molecules of type i and V is the volume of the system.

For a given distance D, the local composition of type i around a central reference species of type j can be directly calculated from coordination numbers according to

$$x_{ij} = \frac{N_{ij}(D)}{\sum_k N_{kj}(D)} = \frac{N_i \int_0^D g_{ij}(r) r^2 dr}{\sum_k N_k (\int_0^D g_{kj}(r) r^2 dr)}$$

where x_{ij} is the local mole fraction of i around j and the sum extends over all species

Then, the association factor can be defined as follows[47]

$$\alpha_{ij}(D) = \frac{x_{ij}(D)}{x_i}$$

where x_i is the bulk mole fraction of species i in the mixture.

The association factors show deviations from random mixing. The association factor parameters α_{ij} takes a value of 1 if there is random mixing of i about j, a value less than 1 if there is a tendency for species j to associate with species other than i relative to the random mixing case, and a value greater than 1 for an attraction between different species i and j relative to that which species j feels with itself or other species. The local association factor α_{ij} can be used to evaluate the relative interaction strength of site–site interactions between species in a mixture. The center of mass RDFs for cation–thiophene, anion–thiophene pairs, and the local association factors for the RDFs pairs are shown Figure 9.

In Figure 9, the first solvation shell peaks for the cation/thiophene pairs is higher than the corresponding peaks of anion/thiophene, indicating that the thiophene associates

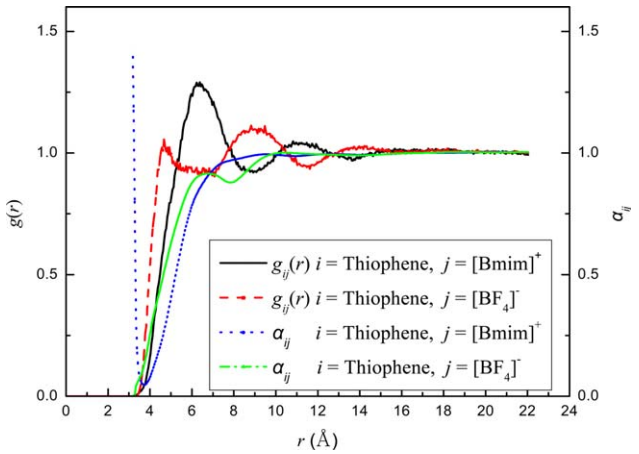

Figure 9. RDFs and association factors for different components in the mixture of xi=0.6 at 318 K and 21.9 kPa.

The sites of i and j represent the center of mass for thiophene and cation/anions, respectively. [Color figure can be viewed in the online issue, which is available at wileyonlinelibrary.com.]

more strongly with the cation than with the anion. To explain any effect of the cation/anion on the relative strength of these interactions, Figure 9 also shows that the cation/thiophene association factors for the mixture is >1 at distances less than 3.23 Å, suggesting that thiophene is able to associate with the cation strongly. While, it is observed that center of mass of anion/thiophene association factors are <1 at less than 10.13 Å and are approximately 1 beyond 11 Å. The association factors describe the local association of thiophene around a central anion, it means that the $[BF_4]$ is not solvated by the thiophene and the interaction between thiophene molecules and anions is not as strong as the interaction of thiophene molecules with itself.

The RDFs only give an average probability distribution between the specified atoms in the three-dimensional direction, but it cannot give a good explanation about local information of interested molecules vicinity at microscopic structure. So, much of the detail information of the local solution structure can be lost as a result of the cancellation of contributions from regions of low and high probability at the same distance but different parts of the local solution structure. In order to overcome these limitations of the RDF, in this article, we also made an analysis of the spatial distribution functions (SDFs). We defined the cation/anion of rIL as a local coordinate system, and provided the probability distribution of thiophene around cations/anions of rIL. In Figures 10 and 11, the spherical molecule structures denote cation and anion, respectively, and the red and yellow regions are the same density distribution at the level. Based on these probability distributions, it can be found the preferred location of thiophene around cation/anion at a given location. In Figure 10, it was found to be a high probability of the sulfur atoms of thiophene near to the alkyl chains of the cation, especially for terminal of butyl. The structure indicates that the thiophene is more easily located near the side chain of the cation, including the butyl and methyl group attached to the imidazolium ring. The findings are in good agreement with the RDFs of sulfur of thiophene around the carbon atoms of cation. Figure 11 shows the 3D distribution of thiophene symmetrically surrounded the $[BF_4]$ anion.

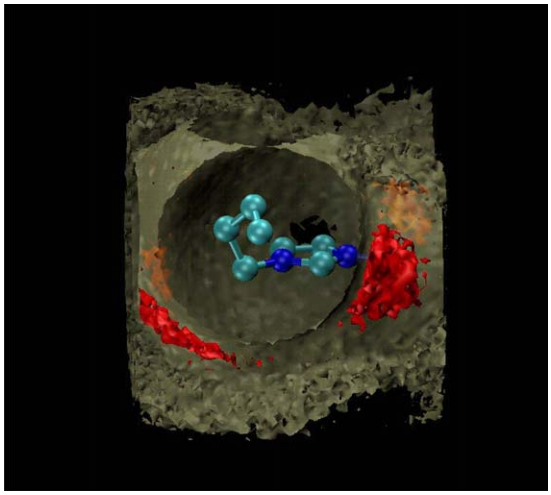

Figure 10. Spatial distribution of thiophene around the [Bmim], the yellow and red regions stand for SDF (isovalue = 1.2 and 3.6, respectively) for the mixture of xi = 0.6 at 318 K and 21.9 kPa.

[Color figure can be viewed in the online issue, which is available at wileyonlinelibrary.com.]

It can clearly be seen that the maximum of the thiophene distribution lies along the directions of pointing toward the fluoride atoms.

We also defined the thiophene as a local coordinate system, and provided the probability distribution of cation atoms around thiophene in Figure 12. It shows that there is clear preference for C6 and C10 atoms of cation to be located closer to thiophene molecule. The results indicate that the length of alkyl chain has a significant effect on the absorption of thiophene in the IL.

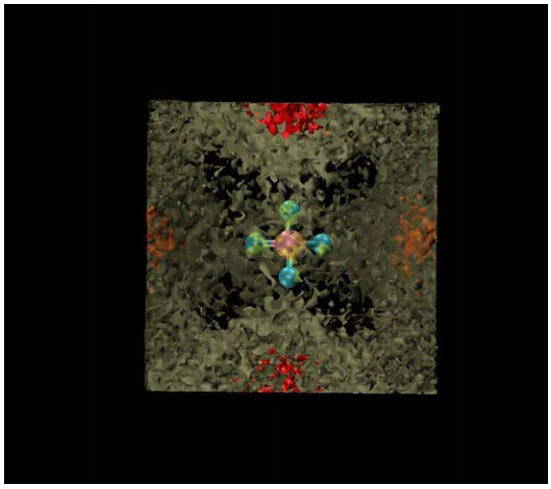

Figure 11. Spatial distribution of thiophene around the [BF4], the yellow and red regions stand for SDF (isovalue = 1.2 and 2.0, respectively) for the mixture of xi = 0.6 at 318 K and 21.9 kPa.

[Color figure can be viewed in the online issue, which is available at wileyonlinelibrary.com.]

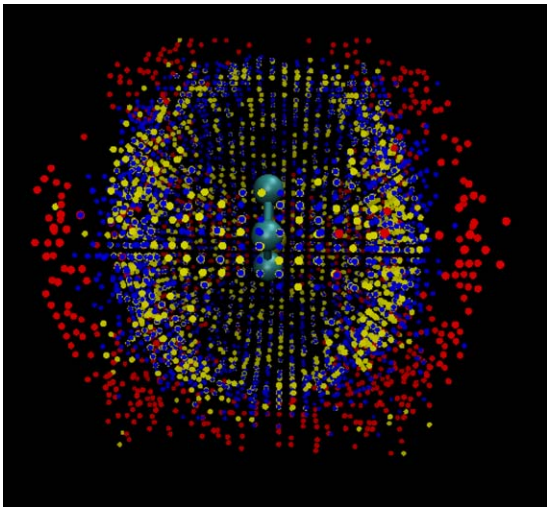

Figure 12. Atom hits of [Bmim] atoms around the thiophene, the red stand for C2 atom, the yellow stand for C6 atom and the blue stand for C10 atom for the mixture of xi = 0.6 at 318 K and 21.9 kPa.

[Color figure can be viewed in the online issue, which is available at wileyonlinelibrary.com.]

Conclusions

Monte Carlo molecular simulations were performed in this study on fluid structure and phase equilibria of the binary system thiophene/[Bmim][BF_4]. A united atom force field was used to examine the phase equilibrium and structural properties through comparing with experimental data. The values obtained for the liquid density and vapor pressure are in very good agreement with the experimental data.

The structure of the liquids was analyzed by computing RDFs and SDFs. It can be found that thiophene is well organized around the terminal carbon atom of the butyl or methyl chain attached to the imidazolium ring of the cation. Thiophene tends to adopt a symmetrical distribution on the anions toward the direction of F atom. The association factors local composition concept also shows that thiophene tends to associate with the cation strongly. The results suggested that changing the length of side chain of cation, may be an effective method to absorb thiophene.

Acknowledgment

The authors thank Prof. Randall Q. Snurr at Northwestern University for reading this manuscript and giving the valuable suggestions. This research work was supported by the Natural Science Foundation of China (Grant No.20806064), Natural Science Foundation of Jiangsu Province, China (BK20131227) and the State Key Laboratory of Materials-Oriented Chemical Engineering, Nanjing University of Technology (KL11-11). Generous allocations of computer time by the ScGrid plan of Supercomputing center of CAS and Testing Center of Yangzhou University.

Literature Cited

1. Song C. An overview of new approaches to deep desulfurization for ultra-clean gasoline, diesel fuel and jet fuel. *Catal. Today*. 2003;86:211–263.
2. Wang L, Yang RT, Sun C. Graphene and other carbon sorbents for selective adsorption of thiophene form liquid fuel. *AIChE J*. 2013;59:29–32.
3. Babich IV, Moulijn JA. Science and technology of novel processes for deep desulfurization of oil refinery streams: a review. *Fuel*. 2003;82:607–631.
4. Yang RT. Adsorbents: Fundamentals and Applications. New York: Wiley, 2003.
5. Bedia J, Ruiz E, de Riva J, Ferro VR, Palomar J, Rodriguez JJ. Optimized ionic liquids for toluene absorption. *AIChE J*. 2013;59:1648–1656.
6. Zhang X, Liu Z, Wang W. Screening of ionic liquids to capture CO_2 by COSMO-RS and experiments. *AIChE J*. 2008;54:2717–2728.
7. Jiang X, Nie Y, Li C, Wang Z. Imidazolium-based alkylphosphate ionic liquids—a potential solvent for extractive desulfurization of fuel. *Fuel*. 2008;87:79–84.
8. Bösmann A, Datsevich L, Jess A, Lauter A, Schmitza C, Wasserscheid P. Deep desulfurization of diesel fuel by extraction with ionic liquids. *Chem Commun*. 2001;23:2494–2495.
9. Zhang SG, Zhang ZC. Novel properties of ionic liquids in selective sulfur removal from fuels at room temperature. *Green Chem*. 2002;4:376–379.
10. Huang CP, Chen BH, Zhang J, Liu ZC, Li YX. Desulfurization of gasoline by extraction with new ionic liquids. *Energy Fuel*. 2004;18(6):1862–1864.
11. Kedra-Krolik K, Fabrice M, Jaubert J. Extraction of thiophene or pyridine from n-heptane using ionic liquids. Gasoline and diesel desulfurization. *Ind Eng Chem Res*. 2011;50:2296–2306.
12. Eßer J, Wasserscheid P, Jess A. Deep desulfurization of oil refinery streams by extraction with ionic liquids. *Green Chem*. 2004;6(7):316–322.
13. Zhang S, Zhang Q, Zhang ZC. Extractive desulfurization and denitrogenation of fuels using ionic liquids. *Ind Eng Chem Res*. 2004;43:614–622.
14. Nie Y, Li CX, Sun AJ, Meng H, Wang ZH. Extractive desulfurization of fuel oil using alkylimidazole and its mixture with dialkylphosphate ionic liquids. *Energy Fuels*. 2006;20:2083–2087.
15. Nie Y, Li CX, Sun AJ, Meng H, Wang ZH. Extractive desulfurization of gasoline using imidazolium-based phosphoric ionic liquids. *Energy Fuels*. 2006;20:2083–2087.
16. Mochizuki Y, Sugawara K. Removal of organic sulfur from hydrocarbon resources using ionic liquids. *Energy Fuels*. 2008;22:3303–3307.
17. Gao HS, Li YG, Wu Y, Luo MF, Li Q, Xing JM, Liu HZ. Extractive desulfurization of fuel using 3-methylpyridinium-based ionic liquids. *Energy Fuels*. 2009;23:2690–2694.
18. Kumar AAP, Banerjee T. Thiophene separation with ionic liquids for desulphurization: a quantum chemical approach. *Fluid Phase Equilib*. 2009;278:1–8.
19. Anantharaj R, Banerjee T. Phase behavior of 1-ethyl-3-methylimidazolium thiocyanate ionic liquid with catalytic deactivated compounds and water at several temperatures: experiments and theoretical predictions. *Int J Chem Eng*. 2011;2011:1–13.
20. Anantharaj R, Banerjee T. Liquid–liquid equilibria for quaternary systems of imidazolium based ionic liquid + thiophene + pyridine + iso-octane at 298.15 K: experiments and quantum chemical predictions. *Fluid Phase Equilib*. 2011;312:20–30.
21. Kedra-Krolik K, Fabrice M, Jaubert J. Extraction of thiophene or pyridine from n-heptane using ionic liquids, gasoline and diesel desulfurization. *Ind. Eng. Chem. Res*. 2011;50:2296–2306.
22. Anantharaj R, Banerjee T. Quantum chemical studies on the simultaneous interaction of thiophene and pyridine with ionic liquids. *AIChE J*. 2011;57:749–764.
23. Su B, Zhang S, Zhang C. Structural elucidation of thiophene interaction with ionic liquids by multinuclear NMR spectroscopy. *J Phys Chem B* 2004;108:19510–19517.
24. Revelli AL, Mutelet F, Jaubert JN. Extraction of benzene or thiophene from n-heptane using ionic liquids. NMR and thermodynamic study. *J Phys Chem B*. 2010;114:4600–4608.
25. Zhou J, Mao J, Zhang S. Ab initio calculations of the interaction between thiophene and ionic liquids. *Fuel Process Technol*. 2008;89:1456–1460.
26. Shah JK, Maginn EJ. A Monte Carlo simulation study of the ionic liquid 1-n-butyl-3-methylimidazolium hexafluorophosphate: liquid structure, volumetric properties and infinite dilution solution thermodynamics of CO_2. *Fluid Phase Equilib*. 2004;195(203):222–223.
27. Andrade JD, Boes ES, Stassen H. Computational study of room temperature molten salts composed by l-alkyl-3-methylimidazolium

cations-force-field proposal and validation. *J Phys Chem B*. 2002;6: 13344–13351.
28. Lubna N, Kamath G, Potoff JJ, Rai N, Siepmann JI. Transferable potentials for phase equilibria. 8. United-atom description for thiols, sulfides, disulfides, and thiophene. *J Phys Chem B*. 2005;109(50): 24100–24107.
29. Martin M, http://towhee.sourceforget.net, 2013.
30. Allen MP, Tildesley DJ. Computer Simulation of Liquids, New York: Oxford University Press, 1987.
31. Siepmann JI, Frenkel D. Configurational-bias Monte Carlo—a new sampling scheme for flexible chains. *Mol Phys*. 1992;75:59–70.
32. Stoppa A, Zech O, Kunz W, Buchner R. The conductivity of imidazolium-based ionic liquids from (−35 to 195)°C. A variation of cation's alkyl chain. *J Chem Eng Data*. 2010;55:1768–1773.
33. Sanmamed YA, Gonzalez-Salagado D, Troncoso J, Cerdeirina CA, Romani L. Viscosity-induced errors in the density determination of room temperature ionic liquids using vibrating tube densitometry. *Fluid Phase Equilib*. 2007;252:96–102.
34. Suarez PAZ, Einloft S, Dullius JEL, Souza RF, Dupont J. Synthesis and physical-chemical properties of ionic liquids based on 1-*n*-butyl-3-methylimidazolium cation. *J Chim Phys*. 1998;95:1626–1639.
35. Sanchez LG, Espel JR, Onink F, Meindersma GW, de Haan AB. Density, viscosity, and surface tension of synthesis grade imidazolium, pyridinium, and pyrrolidinium based room temperature ionic liquids. *J Chem Eng Data*. 2009;54:2803–2812.
36. Prado CER, Freitas LCG. Molecular dynamics simulation of the room-temperature ionic liquid 1-butyl-3-methylimidazolium tetrafluoroborate. *J Mol Struct*. 2007;847:93–100.
37. Yaws CL, Thermodynamic and Physical Property Data, Houston, TX: Gulf Publishing Company, 1992.
38. Morrow TI, Maginn EJ. Molecular dynamics study of the ionic liquid 1-*n*-butyl-3-methylimidazolium hexafluorophosphate. *J Phys Chem B*. 2002;106(49): 12807–12813.
39. Bhargava BL, Balasubramanian S, Klein L. Modelling room temperature ionic liquids. *Chem Commun*. 2008;29:3339–3351.
40. Huo Y, Xia SQ, Yi SZ, Ma PS. Measurement and correlation of vapor pressure of benzene and thiophene with [BMIM][PF_6] and [BMIM][BF_4] ionic liquids. *Fluid Phase Equilib*. 2009;276:46–52.
41. Pádua AAH. *Thermodynamics 2005 Conference*, Portugal: Sesimbra, 2005.
42. Canongia Lopes JN, Costa Gomes MF, Padua AAH. Nonpolar, polar, and associating solutes in ionic liquids. *J Phys Chem B*. 2006; 110:3330–3335.
43. Padua AAH, Costa Gomes MF, Canongia Lopes JNA. Molecular solutes in ionic liquids: a structural perspective. *Acc Chem Res*. 2007;40:1087–1096.
44. Gutel T, Santini CC, PaÇdua AAH, Fenet B, Chauvin Y, Canongia Lopes JN, Bayard F, Costa Gomes MF, Pensado AS. Interaction between the π-system of toluene and the imidazolium ring of ionic liquids: a combined NMR and molecular simulation study. *J Phys Chem B*. 2009;113:170–177.
45. Rowley RL. Statistical Mechanics for Thermophysical Property Calculations, New York: Prentice-Hall, 1994.
46. Jaretun A, Aly G. New local composition model for electrolyte solutions: single solvent, single electrolyte systems. *Fluid Phase Equilib*. 1999;163:175–193.
47. Morrow TI, Maginn EJ. Density, local composition and diffusivity of aqueous choline chloride solutions: a molecular dynamics study. *Fluid Phase Equilib*. 2004;217:97–104.

Manuscript received Apr. 11, 2014, and revision received July 2, 2014.